THE JOURNAL OF BIOLOGICAL CHEMISTRY VOL. 281, NO. 49, pp. 37972–37979, December 8, 2006

Proteolytic Processing of OPA1 Links Mitochondrial Dysfunction to Alterations in Mitochondrial Morphology*

Received for publication, June 26, 2006, and in revised form, September 1, 2006 Published, JBC Papers in Press, September 26, 2006, DOI 10.1074/jbc.M606059200

Stéphane Duvezin-Caubet[‡], Ravi Jagasia[§], Johannes Wagener[‡], Sabine Hofmann[¶], Aleksandra Trifunovic[‖], Anna Hansson[‖], Anne Chomyn[**], Matthias F. Bauer[‡‡], Giuseppe Attardi[**], Nils-Göran Larsson[‖], Walter Neupert[‡], and Andreas S. Reichert[‡1]

From the [‡]Adolf-Butenandt-Institut für Physiologische Chemie, Ludwig-Maximilians-Universität München, Butenandtstrasse 5, 81377 München, Germany, [§]Institute of Developmental Genetics, GSF-National Research Center for Environment and Health, 85764 Munich Neuherberg, Germany, [‖]Department of Laboratory Medicine, Division of Metabolic Diseases, Karolinska Institute, Novum, S-141 86 Stockholm, Sweden, [**]Division of Biology, California Institute of Technology, Pasadena, California 91125, [¶]Institute of Diabetes Research, Academic Hospital Munich-Schwabing, 80804 München, Germany, and [‡‡]Institute of Clinical Chemistry, Molecular Diagnostics, and Mitochondrial Genetics, Academic Hospital Munich-Schwabing, 80804 München, Germany

Many muscular and neurological disorders are associated with mitochondrial dysfunction and are often accompanied by changes in mitochondrial morphology. Mutations in the gene encoding OPA1, a protein required for fusion of mitochondria, are associated with hereditary autosomal dominant optic atrophy type I. Here we show that mitochondrial fragmentation correlates with processing of large isoforms of OPA1 in cybrid cells from a patient with myoclonus epilepsy and ragged-red fibers syndrome and in mouse embryonic fibroblasts harboring an error-prone mitochondrial mtDNA polymerase γ. Furthermore, processed OPA1 was observed in heart tissue derived from heart-specific TFAM knock-out mice suffering from mitochondrial cardiomyopathy and in skeletal muscles from patients suffering from mitochondrial myopathies such as myopathy encephalopathy lactic acidosis and stroke-like episodes. Dissipation of the mitochondrial membrane potential leads to fast induction of proteolytic processing of OPA1 and concomitant fragmentation of mitochondria. Recovery of mitochondrial fusion depended on protein synthesis and was accompanied by resynthesis of large isoforms of OPA1. Fragmentation of mitochondria was prevented by overexpressing OPA1. Taken together, our data indicate that proteolytic processing of OPA1 has a key role in inducing fragmentation of energetically compromised mitochondria. We present the hypothesis that this pathway regulates mitochondrial morphology and serves as an early response to prevent fusion of dysfunctional mitochondria with the functional mitochondrial network.

Mitochondria fulfill a number of essential functions in the eukaryotic cell. One such process is oxidative phosphorylation, a process that generates the vast majority of cellular ATP. Therefore, it is not surprising that many muscular and neurological disorders, various forms of cancer, diabetes, obesity, and aging, are associated with mitochondrial dysfunction (1–6). Interestingly, in many of these diseases or conditions aberrant mitochondrial morphologies are observed (1, 7). Mitochondria in numerous cell types form a large network of interconnected tubules that is maintained by a balance of fission and fusion events (8, 9). Deficiencies in mitochondrial fusion and fission play an important role in various neurodegenerative diseases such as Charcot-Marie-Tooth disease type 2A and 4A, and optic atrophy type 1 (10–13). Furthermore, these dynamic processes apparently are crucial for the cell, *e.g.* in apoptosis (14–18), formation of dendritic spines and synapses (19, 20), and functional complementation of mtDNA mutations by content mixing (21, 22). Fusion of mitochondria, in particular of the inner mitochondrial membrane, depends on the presence of a mitochondrial membrane potential (23–26). Still it is unclear how mitochondrial dysfunction and fragmentation of mitochondria are linked on a molecular level. Here we report on a major molecular player, namely OPA1, in this process.

Mutations in the *OPA1* gene are known to cause hereditary autosomal dominant optic atrophy type I, the most prevalent hereditary neuropathy of the optic nerve occurring with a prevalence of 1:12,000 to 1:50,000, depending on the population (10, 11). The OPA1 protein is required for mitochondrial fusion (27–29). Overexpression of OPA1 in mouse embryo fibroblasts promotes tubulation of mitochondria (28). Down-regulation of OPA1 leads to fragmentation of mitochondria, mitochondrial dysfunction, altered mitochondrial inner membrane morphology, and increased propensity for apoptosis (15, 18, 27, 29, 30). Eight alternatively spliced mRNAs transcribed from the *OPA1* gene and several tissue-specific isoforms of the OPA1 protein were described (31, 32). The ortholog of OPA1 in bakers' yeast, Mgm1, is essential for mitochondrial fusion (33, 34) and is present in two proteolytically matured isoforms, l-Mgm1 and s-Mgm1, both of which are required for function (35). Formation of s-Mgm1 depends on an ATP-dependent mechanism termed alternative topogenesis (36). Therefore, the bioenergetic state of mitochondria was proposed to be linked to their morphology. Here we report that in mouse and human the orthologous protein OPA1 has a key role in linking the bioen-

* This work was supported by the Deutsche Forschungsgemeinschaft/SFB 594-B8 (to A. S. R.), NGFN I/MITOP (to A. S. R. and W. N.), the Friedrich-Baur-Stiftung (to A. S. R.), the Alexander von Humboldt Foundation (to R. J.), the LMU München/FöFoLe (to J. W.), and the National Institutes of Health Grant GM11726 (to A. C.). The costs of publication of this article were defrayed in part by the payment of page charges. This article must therefore be hereby marked "*advertisement*" in accordance with 18 U.S.C. Section 1734 solely to indicate this fact.

[1] To whom correspondence should be addressed. Tel.: 49-89-2180-77100; Fax: 49-89-2180-77093; E-mail: Andreas.Reichert@med.uni-muenchen.de.

ergetic state of mitochondria to mitochondrial morphology, albeit in a mechanistically distinct manner.

EXPERIMENTAL PROCEDURES

Cell Culture and Reagents—HeLa cells, human fibroblasts, immortalized mouse embryonic fibroblast from control (mouse embryonic fibroblast cell lines 13 and 14) and mutator mice (mouse embryonic fibroblast cell lines 2 and 7) (37, 38) and cybrid cell lines (pT1 and pT3) (39) were grown under standard conditions in Dulbecco's modified Eagle's medium containing 4.5 g/liter glucose and 2 mM L-glutamine supplemented with 10% fetal bovine serum, 50 units/ml penicillin, and 50 μg/ml streptomycin. Cell culture reagents were obtained from PAA Laboratories (Cölbe, Germany); CCCP,[2] *o*-phenanthroline, and cycloheximide were purchased from Sigma, and phenylmethylsulfonyl fluoride was from Serva (Germany). The plasmid pMSCV-*Opa1*, encoding a mouse variant of OPA1 corresponding to human spliceform 1, was a kind gift of Luca Scorrano (Padova, Italy) (28). The $DRP1_{K38E}$ N-terminally fused to cyan fluorescent protein (p*ECFP-C1-DVLP*$_{K38E}$) and mitochondrially targeted GFP plasmids (pcDNA3-*OCT:GFP*) were kind gifts of Heidi McBride (Ottawa Heart Institute, Canada). Transient transfections of HeLa cells were performed using Metafectene (Biontex Laboratories, Germany) or FuGENE HD (Roche Applied Science).

Tissue Samples—Heart tissue was obtained from heart-specific TFAM knock-out mice as described earlier (40). Skeletal muscle biopsies were derived from patients diagnosed with respiratory chain disorders (patients 1–10) or control patients (control patients A–D) with no such defects. Informed consent was given by all patients. Patients 1–10 included in this study were previously diagnosed with respiratory chain disorders suffering from mitochondrial encephalomyopathies or isolated myopathies on the basis of clinical, biochemical, morphological, and, in some cases, genetic findings. The activities of the respiratory chain complexes of all control patients were within the normal range. Measurements of rotenone-sensitive NADH-ubiquinone oxidoreductase (complex I), succinate-cytochrome *c* oxidoreductase (complexes II and III). and cytochrome *c* oxidase (complex IV) were determined spectrophotometrically in skeletal muscle homogenates according to Fischer *et al.* (41). Activities were expressed as units per gram of noncollagenous protein and related to the mitochondrial marker enzyme citrate synthase. Homogenates from skeletal muscle biopsies were analyzed by Western blotting, and band intensities were determined densitometrically from the immunoblot.

Antibodies—Anti-OPA1 antibodies were affinity-purified from a rabbit polyclonal serum raised against the C terminus of human OPA1 using the synthetic peptide CDLKKVREIQEK-LDAFIEALHQEK (Pineda Antikörper-Service, Berlin). Antibodies against human MIA40 were raised in rabbits using purified MIA40 fused to maltose-binding protein. Polyclonal rabbit sera against hTim23 and hTim44 were raised as described previously (42). Mouse anti cytochrome *c* (clone 7H8.2C12; BD Biosciences), anti-DRP1 (DLP1 clone 8; BD Biosciences), and anti-β-actin (clone AC-15; Sigma) monoclonal antibodies were used for immunoblotting. The goat anti-AIF (D-20) and rabbit anti-Fis1 sera were purchased from Santa Cruz Biotechnology and IMGENEX, respectively. The anti-Mfn2 serum was a kind gift of Antonio Zorzano (University of Barcelona, Spain).

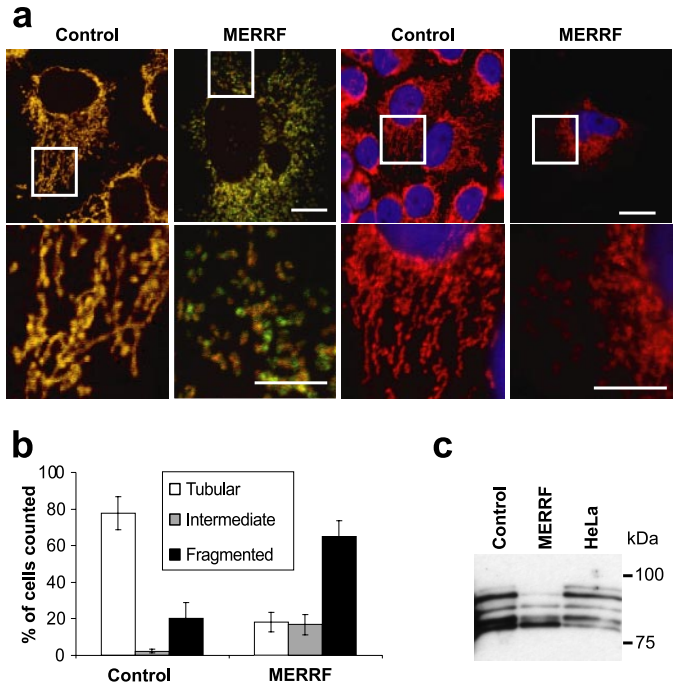

FIGURE 1. **MERRF cybrid cells show fragmentation of mitochondria and alterations in OPA1 isoforms.** MERRF and control cybrid cell lines were cultured, stained with MitoTracker (*red*), fixed, and either immunostained against cytochrome *c* (*green*) or stained with 4′,6-diamidino-2-phenylindole dihydrochloride (*blue*). *a,* merged confocal fluorescence images are shown. *Top,* overview (*scale bar,* 20 μm); *bottom*, indicated box (*scale bar,* 10 μm). *b,* quantification of mitochondrial morphology in cells: *tubular*, at least one mitochondrial tubule of 5 μm or more; *intermediate*, at least one between 0.5 and 5 μm but none more than 5 μm; *fragmented*, none of more than 0.5 μm in length. *c,* OPA1 isoforms in Western blot analysis of total cell extracts. *c*, HeLa cell extracts are shown for comparison.

Fluorescence Microscopy—Live cells were fluorescently labeled with MitoTracker® Red CMXRos (Molecular Probes) for mitochondria or with 4′,6-diamidino-2-phenylindole dihydrochloride (Molecular Probes) for the nucleus after fixation and permeabilization. Immunostaining was carried out with mouse anti-cytochrome *c* monoclonal antibody (clone 6H2.B4; BD Biosciences) and chicken anti-GFP antibody (Aves Lab Inc.). The following secondary antibodies conjugated to fluorescent dyes were used: Alexa Fluor® 488 goat anti-mouse IgG (H+L) (Molecular Probes), Cy3-conjugated donkey anti-mouse IgG (H+L), and fluorescein isothiocyanate-conjugated donkey anti-chicken IgG (Jackson ImmunoResearch). Cells were mounted with Prolong® Gold antifade reagent (Molecular Probes). All treatments were done according to the manufacturers' instructions. Mitochondrial morphology was analyzed by confocal microscopy using a Zeiss LSM 510 (Carl Zeiss Microscopy, Jena, Germany) equipped with a ×63 objective. For all imaging, 512 × 512 pixel images of single confocal planes were acquired and processed with the Bitplane Imaris 4 software. At least 100 cells were analyzed for each slide of each

[2] The abbreviations used are: CCCP, carbonyl cyanide 3-chlorophenylhydrazone; GFP, green fluorescent protein; MERRF, myoclonus epilepsy and ragged-red fibers syndrome; CHX, cycloheximide; MELAS, myopathy encephalopathy lactic acidosis and stroke-like episode.

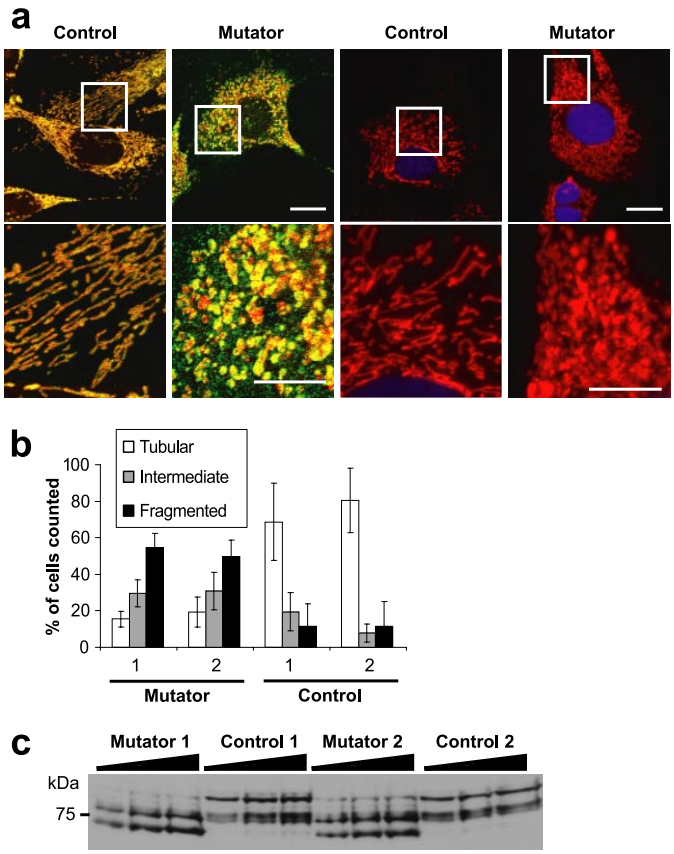

FIGURE 2. **Mutator mouse embryonic fibroblasts show fragmentation of mitochondria and alterations in OPA1 isoforms.** Immortalized mouse embryonic fibroblasts from two control mice and two mutator mice were cultured, stained with MitoTracker (*red*), fixed, and either immunostained against cytochrome *c* (*green*) or stained with 4′,6-diamidino-2-phenylindole dihydrochloride (*blue*). *a,* merged confocal fluorescence images are shown. *Top*, overview (*scale bar,* 20 μm); *bottom*, indicated box, (*scale bar,* 10 μm). *b,* quantification of mitochondrial morphology as in Fig. 1*b*. *c,* OPA1 isoforms in Western blot analysis of total cell extracts.

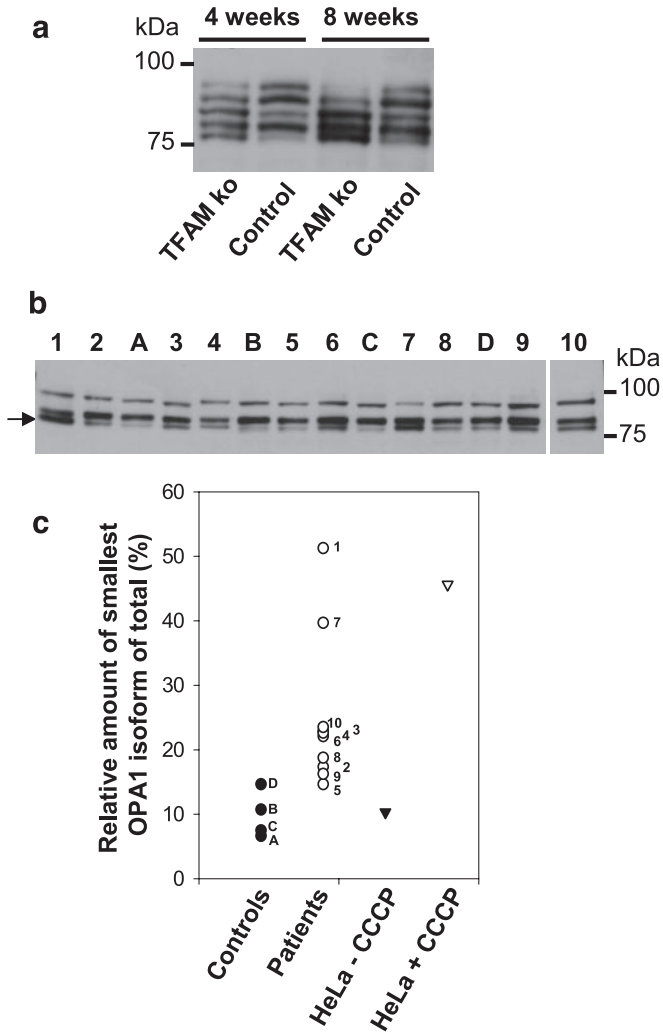

FIGURE 3. **Patterns of OPA1 isoforms are altered in tissue samples exemplary of mitochondrial dysfunction.** *a,* Western blot analysis of OPA1 isoforms of heart tissue from mice with a heart-specific knock-out of TFAM (*TFAM ko*) at 4 or 8 weeks age and of control mice. *b,* homogenates from skeletal muscle biopsies from control individuals (*A–D*) and from patients suffering from respiratory disorders (*patients 1–10*, see Table 1) analyzed by Western blotting for OPA1. The smallest form of OPA1 detected is indicated by an *arrow*. *c,* relative amounts of the smallest OPA1 isoform of all OPA1 isoforms determined densitometrically from *b* and from HeLa cells treated or not for 6 h with CCCP (Fig. 4*b*, *two left lanes*).

condition or cell line. Error bars represent standard deviations calculated from three to five slides.

Pulse-Chase Experiments—HeLa cells were seeded on 6-well plates (10^5 cells per well). One day later, the cells were washed two times with phosphate-buffered saline and starved for 30 min in Dulbecco's modified Eagle's medium without sodium pyruvate, L-methionine, and L-cystine (Invitrogen). Pulse labeling was started by addition of the metabolic labeling reagent (Tran^{35}S-label, MP Biochemicals Europe), and cells were incubated for 2 h 30 min, washed twice with phosphate-buffered saline, and either harvested at that time point or incubated further with complete Dulbecco's modified Eagle's medium supplemented with 10% fetal bovine serum, harvested, lysed in lysis buffer (0.5% Triton X-100, 150 mM NaCl, 10 mM Tris/HCl, 5 mM EDTA, supplemented with complete protease inhibitor mixture purchased from Roche Applied Science), and submitted to immunoprecipitation with OPA1 antibodies and protein A-Sepharose CL-4B beads (Amersham Biosciences). Preimmune serum was used in control experiments. The elution fractions of the different immunoprecipitation experiments were analyzed by Western blotting and digital autoradiography after SDS-PAGE using the same membrane.

Subcellular Fractionation of Cells—Cells were harvested, washed in phosphate-buffered saline supplemented with 5 mM EDTA, and resuspended in 1 ml of RSB buffer (10 mM HEPES (pH 7.5), 1 mM EDTA, 210 mM mannitol, 70 mM sucrose, supplemented with complete protease inhibitor mixture). Cells were broken by six passages through a 26-gauge needle fitted to a 5-ml syringe. Cell pellets from low speed centrifugations (2,000 × *g*, 10 min, 4 °C) were resuspended in RSB buffer and passaged again through a needle as described. This step was repeated 3 to 4 times. The supernatants from low speed centrifugations were pooled and centrifuged again (13,000 × *g*, 10 min, 4 °C) to obtain a crude mitochondrial pellet and a cytosolic supernatant.

RESULTS

MERRF Cybrid Cells Show Fragmentation of Mitochondria and Alterations in OPA1 Isoforms—In a first approach to study the molecular mechanism of fragmentation of mitochondria in

TABLE 1

Genetic and biochemical analysis of mitochondrial function in skeletal muscle biopsies from patients and controls

Patients 1–10 included in this study were previously diagnosed with respiratory chain disorders. A–D represent control patients without such disorders. The activities of the respiratory chain complexes (I to IV) of all controls and patients were determined in skeletal muscle homogenates and are expressed in percent of the lowest limit of the respective reference range. The genetic defect causing the disease is indicated when known. Homogenates from skeletal muscle biopsies were analyzed by Western blotting for OPA1 pattern (Fig. 3*b*). The relative amount of the smallest detected form of OPA1 of all OPA1 isoforms was determined densitometrically from the immunoblot of Fig. 3*b*. The values of this ratio are indicated here and plotted in Fig. 3*c*. MELAS indicates myopathy encephalopathy lactic acidosis and stroke-like episodes.

Samples	Respiratory chain enzyme activities			Genetics	Relative amount of smallest OPA1 isoform of total
					%
A	Normal				6.7
C	Normal				7.5
B	Normal				10.7
D	Normal				14.7
5	I, 10%			Unknown	14.7
9	I, 80%	II/III, 40%	IV, 20%	Unknown	16.3
2			IV, 20%	Unknown	17.3
8	I, 70%	II/III, 60%	IV, 10%	A1541G mutation in *SCO2*	18.7
6	I, 30%			Unknown	22.1
4	I, 30%		IV, 30%	mtDNA depletion	22.7
3	I, 30%	II/III, 80%	IV, 30%	Unknown	22.9
10	I, 50%	II/III, 50%	IV, 20%	mtDNA depletion	23.5
7	I, 50%	II/III, 50%	IV, 80%	MELAS A3243G mutation in tRNA-Leu$^{(UUR)}$	39.7
1	I, 50%	II/III, 50%	IV, 20%	mtDNA depletion	51.2

human diseases, we investigated the role of fusion-promoting OPA1 in a cybrid cell line derived from a MERRF patient suffering from severe myopathy (39). The mtDNA in the cell line contained the A8344G mutation in the tRNA^{Lys} in a nearly homoplasmic manner leading to a substantial impairment of mitochondrial function (39). The cells from the MERRF patient, but not control cells, showed highly fragmented mitochondria (Fig. 1, *a* and *b*). The pattern of the five detected OPA1 protein isoforms was altered in the MERRF cells compared with control cells (Fig. 1*c*). It appears that in the MERRF cells the larger isoforms are reduced compared with the smallest isoform of OPA1. As OPA1 is required for mitochondrial fusion, the observed loss of large OPA1 isoforms may explain the fragmentation of mitochondria in this model system of mitochondrial dysfunction.

Mutator Mouse Embryonic Fibroblasts Show Fragmentation of Mitochondria and Alterations in OPA1 Isoforms—To further substantiate this, we analyzed immortalized mouse embryonic fibroblasts derived from the so-called "mutator mouse" (37, 38). This mouse was generated by a homozygous knock-in of a variant of mtDNA polymerase γ resulting in a phenotype of premature aging. The variant enzyme has much reduced proofreading activity, and mtDNA accumulates random point mutations at a 3–5-fold higher rate than normal leading to severe mitochondrial dysfunction. Mitochondria were extensively fragmented in mutator but not in control cell lines (Fig. 2, *a* and *b*). The levels of the larger OPA1 isoforms were strongly reduced, whereas the levels of the smaller forms were increased in the mutant cells (Fig. 2*c*). These findings suggest that mutations in mtDNA are causative to changes in OPA1 isoform levels and mitochondrial fragmentation.

Patterns of OPA1 Isoforms Are Altered in Tissue Samples Exemplary of Mitochondrial Dysfunction—TFAM is an essential mitochondrial transcription factor also required for mtDNA maintenance. A heart-specific knock-out of TFAM in mice led to a severe depletion of mtDNA in the heart, resulting in cardiomyopathy and altered mitochondrial morphology (40). The pattern of OPA1 isoforms in heart tissue of these mice was changed as compared with controls; the abundance of larger OPA1 isoforms was reduced, whereas that of smaller isoforms was increased (Fig. 3*a*). This was even more pronounced at 8 weeks compared with 4 weeks of age (Fig. 3*a*), consistent with the progression of the cardiomyopathy in those mice (40). This shows that mitochondrial dysfunction resulting from mtDNA depletion is linked to the reduction of larger OPA1 isoforms in the affected tissue. Moreover, the alterations of mitochondrial morphology observed earlier by electron microscopy (40) are likely because of the shift in the levels of OPA1 isoforms.

In addition, we checked whether alterations in the OPA1 isoform pattern are detectable in patients diagnosed with respiratory chain defects. Indeed, an increase of smaller OPA1 isoforms was observed in skeletal muscle from these patients but not from controls (Fig. 3*b*). This was quantified by determining the ratios of the amounts of the smallest OPA1 isoform (*arrow* in Fig. 3*b*) to the total of all OPA1 isoforms (Fig. 3*c*). Besides the shift patients exhibited a much broader variation compared with controls. The patients with mitochondrial DNA depletion syndromes or harboring a MELAS mutation were among those with the highest ratios (Fig. 3*c*, *patients 1* and *7* and Table 1). In none of the controls did we observe such a shift. We conclude that OPA1 isoforms are altered in patients with mitochondrial disorders, in particular those with depletion of or mutations in mtDNA.

Dissipation of the Membrane Potential Leads to Mitochondrial Fragmentation and to Proteolytic Conversion of Larger into Smaller Isoforms of OPA1—Next we asked whether dissipation of the membrane potential is sufficient to trigger changes in the abundance of OPA1 isoforms and whether this coincides with fragmentation of mitochondria. Indeed, treatment of HeLa cells or fibroblasts with the uncoupler CCCP led to fragmentation of mitochondria (Fig. 4*a*; data not shown) consistent with earlier reports (23, 25, 26). Furthermore, this coincided with a dramatic shift of OPA1 isoforms toward the smaller isoforms (Figs. 3*c* and 4*b*). A similar behavior was reported recently in another study performed in parallel (43). Processing is specific to OPA1 as other known fusion and fission components such as Mfn2, Drp1, and Fis1 are not pro-

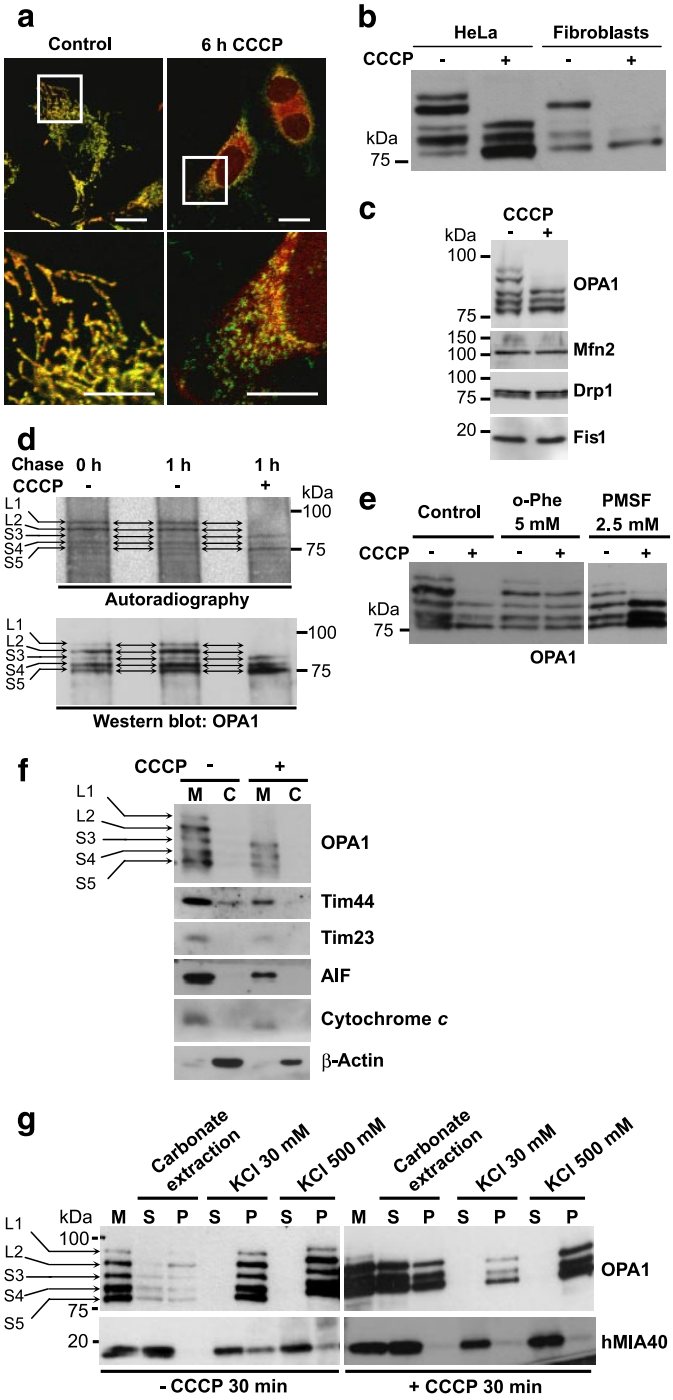

FIGURE 4. **Dissipation of the membrane potential induces mitochondrial fragmentation and concomitant OPA1 processing within mitochondria.** *a,* HeLa cells were treated with CCCP (20 μM) for 6 h, stained with MitoTracker (*red*), fixed, and immunostained against cytochrome *c* (*green*). Merged confocal fluorescence images are shown. *Top,* overview (*scale bar,* 20 μm); *bottom,* indicated box (*scale bar,* 10 μm). *b,* HeLa cells and human fibroblasts were treated with CCCP (20 μM) for 6 h, and total cell extracts were subjected to Western blotting with OPA1 antibodies. *c,* HeLa cells were treated or not with CCCP (20 μM) for 30 min, and total cell lysates were subjected to Western blotting with the indicated antibodies. *d,* pulse-chase experiment. HeLa cells were subjected to radioactive labeling of newly synthesized proteins. After labeling cells were washed, incubated for the indicated time in the absence of radiolabeled amino acids (chase) either in the presence or the absence of CCCP (20 μM). Cells were lysed at indicated times of chase and subjected to immunoprecipitation with antibodies raised against OPA1. Elution fractions were analyzed by digital autoradiography (*top panel*), and the same membrane was subjected to Western blot analysis using Opa1 antibodies (*bottom panel*). The different Opa1 isoforms are indicated by *arrows* and named L1-, L2-, S3-, S4-, and S5-OPA1. *e,* inhibition of OPA1 processing. HeLa cells were preincubated for 10 min with or without the indicated protease inhibitors prior to addition of CCCP (20 μM) or incubation without CCCP, incubated for 25 min, harvested, lysed, and analyzed by Western blotting with OPA1 antibodies. *o-Phe,* mM *o*-phenanthroline; PMSF, phenylmethylsulfonyl fluoride. *f,* OPA1 processing takes place within mitochondria. HeLa cells were treated or not with CCCP (20 μM) for 30 min, harvested, and subjected to subcellular fractionation. Equal portions of the mitochondrial fraction (*M*) and of the cytosolic fraction (*C*) were analyzed by SDS-PAGE and immunoblotted for the indicated proteins. *g,* membrane association of OPA1 isoforms. Isolated mitochondria (100 μg) from HeLa cells treated with CCCP for 30 min (*right*) or untreated (*left*) were extracted either with 30 or 500 mM KCl after sonication or with 0.1 M sodium carbonate (pH 11). Pellets were recovered by centrifugation, and 25% of each fraction, pellet (*P*), and supernatant (*S*) was analyzed by SDS-PAGE and immunoblotted for the indicated proteins. *hMia40*, a soluble protein of the intermembrane space, serves as control.

cessed (Fig. 4*c*). To test whether the two larger OPA1 isoforms are converted into the smaller ones upon dissipation of the membrane potential, we performed metabolic, radioactive pulse labeling of HeLa cells followed by a chase in the absence or presence of CCCP for 1 h. We could confirm that indeed the two larger OPA1 isoforms (L1- and L2-OPA1) are converted into the smaller ones (S3-, S4-, and S5-OPA1), in particular into S3- and S5-OPA1 (Fig. 4*d*). This is apparently because of proteolytic cleavage of the larger forms because this process was blocked in the presence of the protease inhibitor *o*-phenanthroline (Fig. 4*e*). Processing of OPA1 occurs within mitochondria because all OPA1 isoforms detected remain in the mitochondrial fraction and are not released to the cytosol after subcellular fractionation (Fig. 4*f*). Furthermore, the smaller isoforms produced could be extracted from mitochondria with detergent-free buffer with a higher efficiency than the larger forms suggesting that the larger forms are integral membrane protein isoforms, and the shorter ones are only peripherally attached to the membrane (Fig. 4*g*). Other mitochondrial proteins, including three intermembrane space proteins (cytochrome *c*, AIF, and hMIA40), are not processed supporting further that processing is specific for OPA1 (Fig. 4, *f* and *g*). Fragmentation of mitochondria occurred rapidly within 15–30 min after addition of CCCP (Fig. 5, *a* and *b*). This is because of a block in mitochondrial fusion as shown earlier (23, 26). Processing of OPA1 took place within the same narrow time frame (Fig. 5*c*). Impairment of fusion of mitochondria may therefore be due to rapid inactivation of OPA1 by proteolysis of larger isoforms. Moreover, upon removal of CCCP, normal mitochondrial morphology was recovered, and this coincided with the reappearance of larger isoforms of OPA1 (Fig. 5, *a*–*c*). Mitochondrial fragmentation and OPA1 processing are not accompanied by cytochrome *c* release in this or in any of the investigated models of mitochondrial dysfunction (Figs. 1*a*, 2*a*, and 4*e* and data not shown). This suggests that mitochondrial fragmentation *per se* does not result in apoptosis consistent with an earlier report (15).

Mitochondrial Fragmentation and OPA1 Processing Are Causally Linked—Mitochondrial fragmentation after dissipation of the membrane potential is not dependent on protein synthesis, whereas recovery of mitochondrial fusion after reestablishing a membrane potential is (26). We asked whether OPA1 processing and resynthesis of OPA1 isoforms, respec-

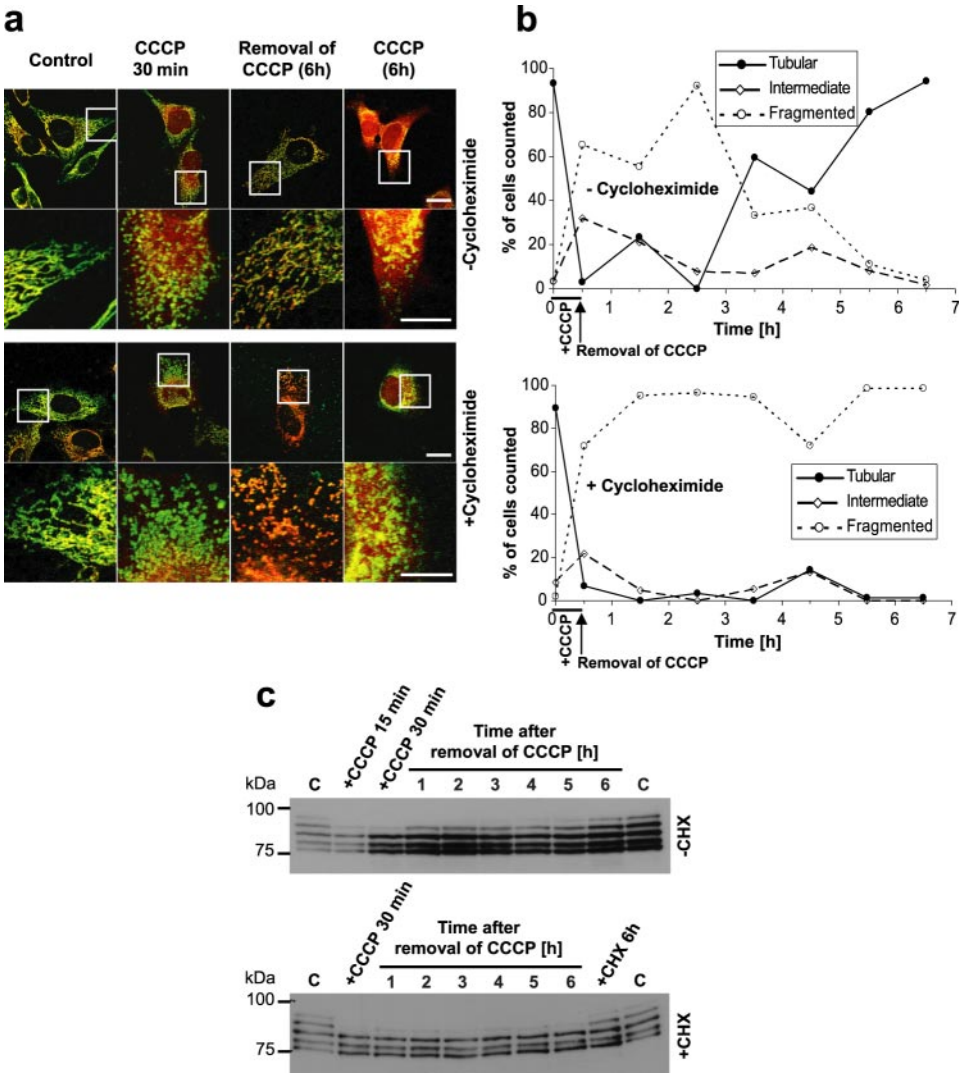

FIGURE 5. **Proteolytic processing and resynthesis of large OPA1 isoforms parallel dynamic changes of mitochondrial morphology.** Cells were treated or not (*Control*) with CCCP (20 μM) for 30 min, washed, and incubated with medium lacking CCCP for the indicated time periods, or CCCP (20 μM) was left for 6 h. In parallel, these experiments were performed in the presence of CHX (175 μg/ml). Cells were stained with MitoTracker (*red*), fixed, and immunostained with cytochrome *c* antibodies (*green*). *a,* merged confocal fluorescence images are shown. *Top,* overview (*scale bar,* 20 μm); *bottom*, indicated box (*scale bar,* 10 μm). *b,* quantification of mitochondrial morphology as in Fig. 1*b*. *c,* OPA1 isoforms in Western blot analysis of total cell extracts. Extracts of untreated cells (*C*) and of cells treated for 6 h with cycloheximide alone (+*CHX* 6 h) were used as controls.

tively, could explain these earlier observations. The protein synthesis inhibitor cycloheximide (CHX) did not interfere with fragmentation and OPA1 processing (Fig. 5, *a–c*). This indicates that fragmentation of mitochondria and activation of OPA1 cleavage are independent of protein synthesis. However, recovery of a tubular mitochondrial network as well as the parallel reappearance of larger OPA1 isoforms was impaired in the presence of CHX (Fig. 5, *a–c*). Therefore, mitochondrial fragmentation and the shift of OPA1 isoforms are not reversible without ongoing protein synthesis consistent with the explanation that a proteolytic inactivation of OPA1 causes mitochondrial fragmentation.

To show the causal and specific role of OPA1 in this process, we decided to check whether OPA1 overexpression can block uncoupler-induced fragmentation. Indeed, fragmentation of mitochondria after CCCP treatment was largely prevented upon overexpression of OPA1 (Fig. 6, *a* and *b*). This suggests that OPA1 is directly involved in the fragmentation of mitochondria induced after loss of the mitochondrial membrane potential. A similar effect was observed after the expression of a dominant-negative variant of DRP1 ($DRP1_{K38E}$) that prevents fission of mitochondria (Fig. 6, *a* and *b*). To check whether overexpression of OPA1 or of a dominant-negative variant of DRP1 ($DRP1_{K38E}$) affects the rate of uncoupler-induced conversion of large OPA1 isoforms into smaller OPA1 isoforms, we performed a pulse-chase experiment. Indeed, overexpression of OPA1 slowed down the processing of OPA1 as indicated by the prolonged presence of L1- and L2-OPA1 when compared with the control overexpression of GFP or of $DRP1_{K38E}$ (Fig. 6*c*). This effect may even be underestimated also because endogenous OPA1 from about 50% of nontransfected cells contributes to the signal. Thus, additional expression of large isoforms of OPA1 blocks CCCP-induced mitochondrial fragmentation consistent with the proposed fusion-promoting activity of a large but not a short OPA1 isoform (43). A dominant-negative variant of DRP1 ($DRP1_{K38E}$) does not affect the rate of OPA1 processing but blocks mitochondrial fragmentation (Fig. 6, *a–c*). Thus, the fragmentation that occurs by a block of mitochondrial fusion depends on the normal DRP1-dependent fission pathway. However, processing of OPA1 appears to occur independently from ongoing mitochondrial fission.

DISCUSSION

The processes of mitochondrial damage leading to dysfunction, breakdown of mitochondrial bioenergetic competence, and mitochondrial fragmentation are linked through a cascade of reactions. Here we have identified a central molecular player, namely OPA1, that links changes in mitochondrial morphology with mitochondrial dysfunction. Our conclusions are based on a wide variety of established model systems and patient material exemplary for MERRF, MELAS, mtDNA depletion syndrome, dilated cardiomyopathy, diseases with respiratory deficiencies of unknown origin, and aging. We put forward an hypothesis that describes how this cascade is organized. Mito-

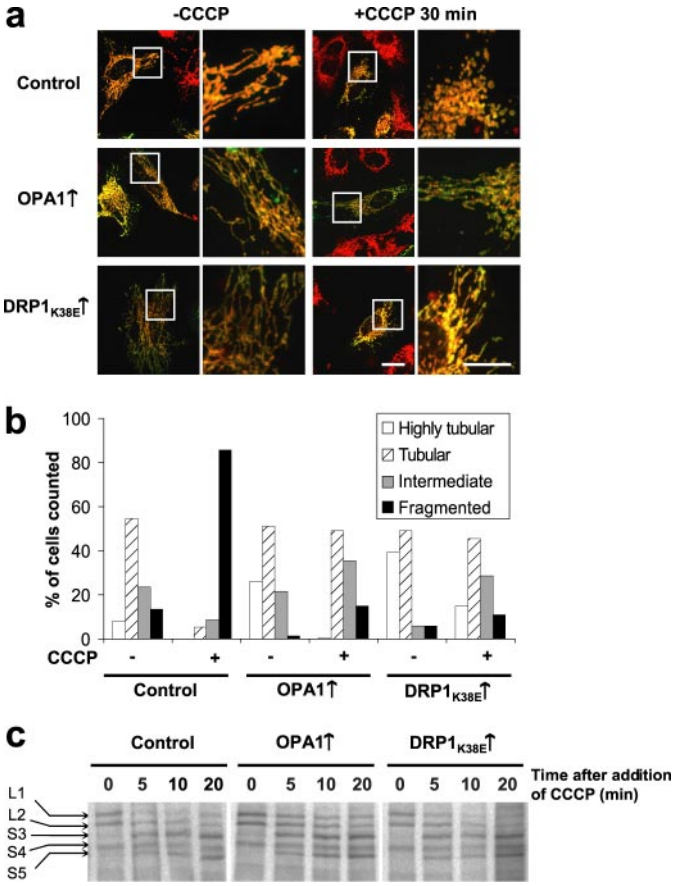

FIGURE 6. **Mitochondrial fragmentation and OPA1 processing are causally linked.** *a,* HeLa cells were transfected with a plasmid expressing mitochondrial GFP (*control*) or co-transfected with this plasmid and a plasmid expressing either a mouse variant of OPA1 corresponding to human splice-form 1 (*OPA1* ↑) or a dominant-negative variant of DRP1 (*DRP1$_{K38E}$* ↑). 36 h after transfection, cells were treated or not with CCCP for 30 min, fixed, and immunostained with GFP (*green*) and cytochrome *c* antibodies (*red*). Merged confocal fluorescence images are shown. *Left,* overview (*scale bar,* 20 μm); *right*, indicated box (*scale bar,* 10 μm). *b,* mitochondrial morphology of mitochondrial GFP-positive cells was quantified. Cells with at least one highly elongated mitochondrion of more than 10 μm (highly tubular) were quantified in addition to those classes described in Fig. 1*b*. *c,* pulse-chase experiment. HeLa cells were transfected as described in *a*. 24 h after transfection, cells were subjected to radioactive labeling and subsequent CCCP treatment during the chase period as described in Fig. 4*d*. At indicated times after addition of CCCP, cells were washed, harvested, lysed, and subjected to immunoprecipitation with antibodies raised against OPA1 in the presence of 5 mM *o*-phenanthroline, 10 mM EDTA. OPA1 isoforms in the elution fractions were separated by SDS-PAGE and analyzed by digital autoradiography.

chondrial dysfunction leads to impairment of bioenergetic competence of mitochondria. This results in reduced membrane potential and ATP production. In such compromised mitochondria, a proteolytic processing of large to small isoforms of OPA1 is activated. As a consequence, fusion of mitochondria is blocked, and due to ongoing mitochondrial fission dysfunctional mitochondria are segregated from the network of intact mitochondria.

A key element of the mechanism proposed here is the regulatory inactivation of fusion-promoting OPA1 by proteolytic cleavage. In the case of the homolog of OPA1 in yeast, Mgm1, lack of either of the proteolytically generated large or small isoforms leads to impairment of mitochondrial fusion (35, 36, 44). We propose that, in a similar way, loss of the two larger isoforms of OPA1 in humans leads to a deficiency in mitochondrial fusion. This is strongly supported by the following observations. 1) OPA1 is required for mitochondrial fusion (27–29). 2) Mitochondrial fusion is blocked after treatment with uncoupler *in vivo* and *in vitro* (23, 25, 26, 43, 45). 3) Both OPA1 processing after uncoupler treatment as well as resynthesis of OPA1 after removal of uncoupler occur in the same time frame as fragmentation and refusion of mitochondria. 4) Overexpression of OPA1 blocks uncoupler-induced fragmentation of mitochondria and slows down processing of large OPA1 isoforms. 5) In particular, the large isoform of OPA1 but not the short isoform was shown to promote mitochondrial fusion (43).

In yeast, mitochondrial dysfunction causes a deficiency in the import of the Mgm1 precursor. Consequently, formation of the small isoform and mitochondrial fusion are impaired (36). In humans, mitochondrial dysfunction is sensed in a different fashion, which is independent of protein synthesis and consequently protein import into mitochondria. Still, this leads to the specific, rapid, and intramitochondrial inactivation of the orthologous effector protein, OPA1.

We propose that this fast and sensitive molecular mechanism that connects mitochondrial functionality and morphology separates dysfunctional from functional mitochondria. This serves mainly two purposes highly relevant to the progression of mitochondrial diseases and neurodegenerative disorders. First, it would reduce further damaging of mtDNA by reactive oxygen species by the spatial separation of damaged mitochondria from the intact tubular network. Second, it would enable the removal of dysfunctional mitochondria by autophagy or more specifically mitophagy. In principle, mitophagy was shown to be increased in some systems of mitochondrial dysfunction (46–48). OPA1-dependent counter-selection of damaged mitochondria is an intracellular process that does not depend on cell division-based selection. It is therefore of particular importance in the aging process and in post-mitotic tissues. Indeed, predominantly these tissues are affected in myopathies and neurodegenerative disorders caused by mitochondrial dysfunction. Interestingly, mutations in OPA1 are known to be causative to hereditary optic atrophy type 1 (10, 11). Therefore, impairment of OPA1 function may result in impaired separation of damaged mitochondria contributing to the pathomechanism of this neurodegenerative disorder. This, however, does not exclude that impairment of mitochondrial fusion leads to a reduced mitochondrial membrane potential, low respiration rate, slow cell growth, and increased susceptibility to apoptosis by other mechanisms as proposed earlier (29).

Acknowledgments—We thank Drs. Luca Scorrano and Heidi McBride for plasmids, Prof. Antonio Zorzano for antibodies, Iris Haag for technical assistance, and Drs. Juan Alfonzo and Doron Rapaport for comments on the manuscript.

REFERENCES

1. Wallace, D. C. (2005) *Annu. Rev. Genet.* **39,** 359–407
2. Shoubridge, E. A. (2001) *Hum. Mol. Genet.* **10,** 2277–2284
3. Smeitink, J. A., Zeviani, M., Turnbull, D. M., and Jacobs, H. T. (2006) *Cell Metab.* **3,** 9–13
4. Modica-Napolitano, J. S., and Singh, K. K. (2004) *Mitochondrion* **4,**

755–762
5. Orth, M., and Schapira, A. H. (2001) *Am. J. Med. Genet.* **106,** 27–36
6. DiMauro, S., and Schon, E. A. (2003) *N. Engl. J. Med.* **348,** 2656–2668
7. DiMauro, S., Bonilla, E., Zeviani, M., Nakagawa, M., and DeVivo, D. C. (1985) *Ann. Neurol.* **17,** 521–538
8. Nunnari, J., Marshall, W. F., Straight, A., Murray, A., Sedat, J. W., and Walter, P. (1997) *Mol. Biol. Cell* **8,** 1233–1242
9. Okamoto, K., and Shaw, J. M. (2005) *Annu. Rev. Genet.* **39,** 503–536
10. Alexander, C., Votruba, M., Pesch, U. E., Thiselton, D. L., Mayer, S., Moore, A., Rodriguez, M., Kellner, U., Leo-Kottler, B., Auburger, G., Bhattacharya, S. S., and Wissinger, B. (2000) *Nat. Genet.* **26,** 211–215
11. Delettre, C., Lenaers, G., Griffoin, J. M., Gigarel, N., Lorenzo, C., Belenguer, P., Pelloquin, L., Grosgeorge, J., Turc-Carel, C., Perret, E., Astarie-Dequeker, C., Lasquellec, L., Arnaud, B., Ducommun, B., Kaplan, J., and Hamel, C. P. (2000) *Nat. Genet.* **26,** 207–210
12. Zuchner, S., Mersiyanova, I. V., Muglia, M., Bissar-Tadmouri, N., Rochelle, J., Dadali, E. L., Zappia, M., Nelis, E., Patitucci, A., Senderek, J., Parman, Y., Evgrafov, O., Jonghe, P. D., Takahashi, Y., Tsuji, S., Pericak-Vance, M. A., Quattrone, A., Battaloglu, E., Polyakov, A. V., Timmerman, V., Schroder, J. M., Vance, J. M., and Battologlu, E. (2004) *Nat. Genet.* **36,** 449–451
13. Niemann, A., Ruegg, M., La Padula, V., Schenone, A., and Suter, U. (2005) *J. Cell Biol.* **170,** 1067–1078
14. Karbowski, M., Lee, Y. J., Gaume, B., Jeong, S. Y., Frank, S., Nechushtan, A., Santel, A., Fuller, M., Smith, C. L., and Youle, R. J. (2002) *J. Cell Biol.* **159,** 931–938
15. Lee, Y. J., Jeong, S. Y., Karbowski, M., Smith, C. L., and Youle, R. J. (2004) *Mol. Biol. Cell* **15,** 5001–5011
16. Frank, S., Gaume, B., Bergmann-Leitner, E. S., Leitner, W. W., Robert, E. G., Catez, F., Smith, C. L., and Youle, R. J. (2001) *Dev. Cell* **1,** 515–525
17. Jagasia, R., Grote, P., Westermann, B., and Conradt, B. (2005) *Nature* **433,** 754–760
18. Arnoult, D., Grodet, A., Lee, Y. J., Estaquier, J., and Blackstone, C. (2005) *J. Biol. Chem.* **280,** 35742–35750
19. Verstreken, P., Ly, C. V., Venken, K. J., Koh, T. W., Zhou, Y., and Bellen, H. J. (2005) *Neuron* **47,** 365–378
20. Li, Z., Okamoto, K., Hayashi, Y., and Sheng, M. (2004) *Cell* **119,** 873–887
21. Nakada, K., Inoue, K., Ono, T., Isobe, K., Ogura, A., Goto, Y. I., Nonaka, I., and Hayashi, J. I. (2001) *Nat. Med.* **7,** 934–940
22. Ono, T., Isobe, K., Nakada, K., and Hayashi, J. I. (2001) *Nat. Genet.* **28,** 272–275
23. Malka, F., Guillery, O., Cifuentes-Diaz, C., Guillou, E., Belenguer, P., Lombes, A., and Rojo, M. (2005) *EMBO Rep.* **6,** 853–859
24. Meeusen, S., McCaffery, J. M., and Nunnari, J. (2004) *Science* **305,** 1747–1752
25. Ishihara, N., Jofuku, A., Eura, Y., and Mihara, K. (2003) *Biochem. Biophys. Res. Commun.* **301,** 891–898
26. Legros, F., Lombes, A., Frachon, P., and Rojo, M. (2002) *Mol. Biol. Cell* **13,** 4343–4354
27. Olichon, A., Baricault, L., Gas, N., Guillou, E., Valette, A., Belenguer, P., and Lenaers, G. (2003) *J. Biol. Chem.* **278,** 7743–7746
28. Cipolat, S., de Brito, O. M., Dal Zilio, B., and Scorrano, L. (2004) *Proc. Natl. Acad. Sci. U. S. A.* **101,** 15927–15932
29. Chen, H., Chomyn, A., and Chan, D. C. (2005) *J. Biol. Chem.* **280,** 26185–26192
30. Griparic, L., van der Wel, N. N., Orozco, I. J., Peters, P. J., and van der Bliek, A. M. (2004) *J. Biol. Chem.* **279,** 18792–18798
31. Satoh, M., Hamamoto, T., Seo, N., Kagawa, Y., and Endo, H. (2003) *Biochem. Biophys. Res. Commun.* **300,** 482–493
32. Olichon, A., Emorine, L. J., Descoins, E., Pelloquin, L., Brichese, L., Gas, N., Guillou, E., Delettre, C., Valette, A., Hamel, C. P., Ducommun, B., Lenaers, G., and Belenguer, P. (2002) *FEBS Lett.* **523,** 171–176
33. Wong, E. D., Wagner, J. A., Scott, S. V., Okreglak, V., Holewinske, T. J., Cassidy-Stone, A., and Nunnari, J. (2003) *J. Cell Biol.* **160,** 303–311
34. Sesaki, H., Southard, S. M., Yaffe, M. P., and Jensen, R. E. (2003) *Mol. Biol. Cell* **14,** 2342–2356
35. Herlan, M., Vogel, F., Bornhövd, C., Neupert, W., and Reichert, A. S. (2003) *J. Biol. Chem.* **278,** 27781–27788
36. Herlan, M., Bornhövd, C., Hell, K., Neupert, W., and Reichert, A. S. (2004) *J. Cell Biol.* **165,** 167–173
37. Trifunovic, A., Wredenberg, A., Falkenberg, M., Spelbrink, J. N., Rovio, A. T., Bruder, C. E., Bohlooly, Y. M., Gidlof, S., Oldfors, A., Wibom, R., Tornell, J., Jacobs, H. T., and Larsson, N. G. (2004) *Nature* **429,** 417–423
38. Trifunovic, A., Hansson, A., Wredenberg, A., Rovio, A. T., Dufour, E., Khvorostov, I., Spelbrink, J. N., Wibom, R., Jacobs, H. T., and Larsson, N. G. (2005) *Proc. Natl. Acad. Sci. U. S. A.* **102,** 17993–17998
39. Chomyn, A., Meola, G., Bresolin, N., Lai, S. T., Scarlato, G., and Attardi, G. (1991) *Mol. Cell. Biol.* **11,** 2236–2244
40. Hansson, A., Hance, N., Dufour, E., Rantanen, A., Hultenby, K., Clayton, D. A., Wibom, R., and Larsson, N. G. (2004) *Proc. Natl. Acad. Sci. U. S. A.* **101,** 3136–3141
41. Fischer, J. C., Ruitenbeek, W., Gabreels, F. J., Janssen, A. J., Renier, W. O., Sengers, R. C., Stadhouders, A. M., ter Laak, H. J., Trijbels, J. M., and Veerkamp, J. H. (1986) *Eur. J. Pediatr.* **144,** 441–444
42. Bauer, M. F., Gempel, K., Reichert, A. S., Rappold, G. A., Lichtner, P., Gerbitz, K. D., Neupert, W., Brunner, M., and Hofmann, S. (1999) *J. Mol. Biol.* **289,** 69–82
43. Ishihara, N., Fujita, Y., Oka, T., and Mihara, K. (2006) *EMBO J.* **25,** 2966–2977
44. Sesaki, H., Southard, S. M., Hobbs, A. E., and Jensen, R. E. (2003) *Biochem. Biophys. Res. Commun.* **308,** 276–283
45. Meeusen, S. L., and Nunnari, J. (2005) *Curr. Opin. Cell Biol.* **17,** 389–394
46. Priault, M., Salin, B., Schaeffer, J., Vallette, F. M., di Rago, J. P., and Martinou, J. C. (2005) *Cell Death Differ.* **12,** 1613–1621
47. Lyamzaev, K. G., Pletjushkina, O. Y., Saprunova, V. B., Bakeeva, L. E., Chernyak, B. V., and Skulachev, V. P. (2004) *Biochem. Soc. Trans.* **32,** 1070–1071
48. Skulachev, V. P., Bakeeva, L. E., Chernyak, B. V., Domnina, L. V., Minin, A. A., Pletjushkina, O. Y., Saprunova, V. B., Skulachev, I. V., Tsyplenkova, V. G., Vasiliev, J. M., Yaguzhinsky, L. S., and Zorov, D. B. (2004) *Mol. Cell. Biochem.* **256,** 341–358